Journal of Alloys and Compounds, 195 (1993) 195–198
JALCOM 7446

Thin films of (RE)$Ba_2Cu_3O_7$ *in-situ* epitaxially grown by laser ablation : crystalline structure, resistivity and critical exponents of temperature dependent critical currents.

G. Dousselin[a], Y. Pellan[a], C. Thivet[b], M. Guilloux-Viry[b], J. Padiou[b], S. Robinet[a] and A. Perrin[b]

[a]Laboratoire de Physique des Solides, URA CNRS 786, INSA de Rennes, 20 Avenue des Buttes de Coësmes, 35043 Rennes cedex, France

[b]Laboratoire de Chimie du Solide et Inorganique Moléculaire, URA CNRS 1495, Université de Rennes I, Avenue du Général Leclerc, 35042 Rennes cedex, France

Abstract

c-axis thin films of (Rare-Earth)$Ba_2Cu_3O_7$, (RE)BCO, superconductors have been epitaxially grown by laser ablation. High crystalline quality has been revealed by electron channeling patterns (ECP). Superconducting properties of as-deposited films have been determined by resistive and inductive measurements before patterning. Transport critical current densities of (RE = Y, Eu, Ho)BCO samples have been measured. Ho and Eu samples behave as homogeneous superconductors : $Jc \propto (1-t)^{3/2}$. Discrepancies with power-law variations can be overcome when considering that thermally activated flux - lines motion governs the Jc's.

1. Introduction

Thin films of high quality superconducting oxides are now currently obtained from different deposition processes for technical applications [1]. We routinely deposit epitaxially grown YBCO films onto various substrates by laser ablation [2]. For microwaves applications, which are expected soon, specific substrates are required. At present, considering the dielectric and structural properties, MgO appears to be a good candidate as substrate.

Taking into account the large misfit between 1:2:3 structures and MgO, we presently try to take advantage of unit-cell variations in (RE)BCO materials. However, dislocations and spiral growth structures have been observed on as-deposited films which are susceptible to act as pinning centers for flux line motion, thus governing the critical current densities in transport current experiments.

2. Film deposition and characterization

Thin films have been grown *in-situ* by laser ablation from a 1:2:3 home made target at a temperature in the range 720-770° C, under oxygen pressure (0.3 mbar) on single-crystal substrates such as (100) MgO, (100) and (110)$SrTiO_3$. A detailed processing description has been previously reported [2].

(110) and (103) YBCO films have been epitaxially grown on (110)$SrTiO_3$ [3] and c-axis films on (100)$SrTiO_3$ substrates [2]. (RE)BCO (RE = Y, Eu, Gd, Ho) thin films deposited at 750° C on (100) MgO substrates are c-axis oriented as characterized by standard θ-2θ x-ray diffractometry and show narrow rocking curves, characteristic of a good crystallinity along the growth direction [4].

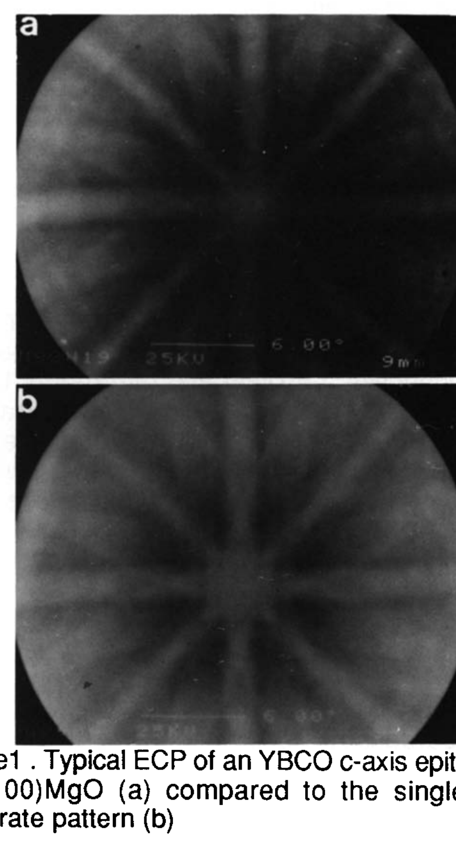

Figure1 . Typical ECP of an YBCO c-axis epitaxial film on (100)MgO (a) compared to the single-crystal substrate pattern (b)

The epitaxy of the films (i.e. alignment of the film

Table 1. Electrical and superconducting properties of (RE)BCO samples

Sample	$T_c(0)$ (K)	ρ_{100K} ($\mu\Omega$.cm)	ρ_{100}/ρ_{300}	$J_c(77)$ A.cm^{-2}	$J_c(0)$ A.cm^{-2}	U_0 meV	α	v_0 m.s^{-1}
L228Y	82.6 ± 0.2	132	0.38	1.6 10^5	10^7	42	5 10^{-4}	6
L259Eu	84.9 ± 0.2	82	0.34	6 10^5	10^7	78	2 10^{-4}	15
L260Ho	86.3 ± 0.2	182	0.38	3 10^5	4.3 10^6	79	10^{-3}	3

crystalline axes with those of the substrate) is verified by *in-situ* reflection high energy electron diffraction (RHEED) [4], *ex-situ* oscillating crystal x-ray diffraction [3] and electron channeling patterns (ECP) [5]. The latter is very sensitive to slight in-plane misalignment of the films : patterns obtained on films deposited on (100) MgO are sharp, as can be seen on Fig. 1, thus demonstrating the high structural quality of our samples. For various rare earths, the ECP are found similar, therefore denoting quasi-identical quality of the films from a structural point of view. The other usual structural characterizations do not show other differences. Critical temperatures, Tc (R = 0), between 85 and 90 K and ΔTc around 1K (resistively and inductively measured) are routinely obtained. Some variations in Tc with regard to the ionic radius of the involved rare-earth seem to be observed, in agreement with results on bulk samples [6]. Under the same deposition conditions, at ~ 750°C, Y, Gd and Ho films have nearly the same Tc (R = 0), typically 87 K, whereas the critical temperature of EuBCO films can reach 90 K.

3. Transport J_c measurements

The resistivity versus temperature ρ(T) and critical current density Jc(T) have been investigated, especially in the temperature range 65 to 90 K, for three given samples selected on the basis of their narrow inductive transition and referred as L228Y, L259Eu and L260Ho respectively. Standard lithography techniques were used to pattern the films into a four probe geometry, the structure consisting of a 200 μm long and 7.5 μm wide stripe. Thermal evaporation of Ag metal pads, together with an "*in-situ*" ion-beam precleaning operation, allowed us to obtain contact resistances $R_\square$ = 10^{-5} Ω.cm^2, without any further annealing step. This is an important feature of our operating process, fully compatible with lift-off delineation operations in metallic contact fabrication. Table I summarizes the electrical and superconducting properties of the samples under study. Fig. 2 displays the results of the measured transport critical current density Jc(T) as a function of temperature for the Y, Eu and Ho films.

The critical currents were taken with a 0.5 μV voltage criterion from the I(V) characteristics, corresponding to a critical electric field Ec = 2.5 10^{-5} V·cm^{-1}. The critical Tc(0)'s were deduced from the Jc(T) and ρ(T) curves in the zero value limit, within a

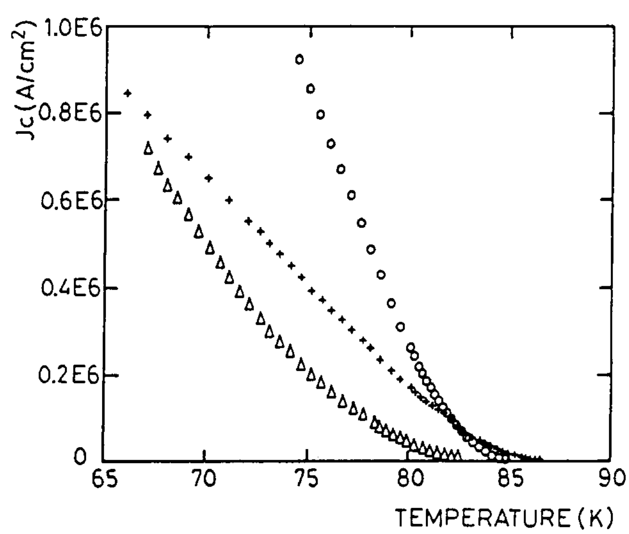

Figure 2. Temperature dependence of J_c for (Δ) = Y, (o) = Eu, (+) = Ho samples

few tenths of degree (≤ 0.2 K) as shown in Fig. 3. In the absence of external magnetic field, we obtained typical values Jc (77) = 3 - 6 10^5 A.cm^{-2}, Tc(0) = 84.9 - 86.3 K for the Eu and Ho samples, the Y sample being of poorer quality with Tc(0) = 82.6 K and Jc(77) = 1.6 10^5 A.cm^{-2}. The resistance ratios ρ(100)/ρ(300) = 0.34 - 0.38 are similar for the three samples.

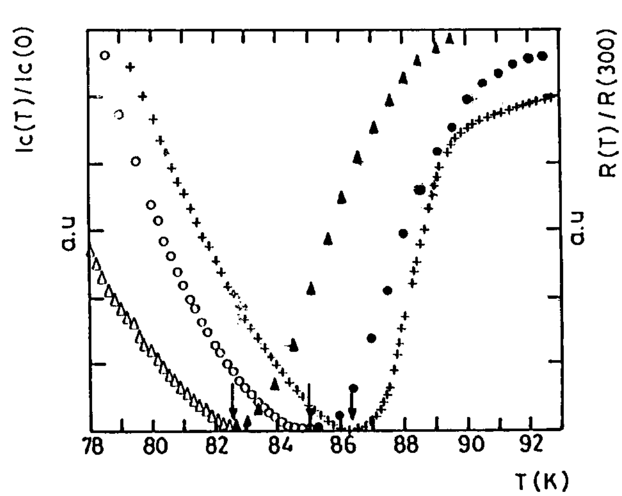

Figure 3. Critical temperature determination from reduced resistance and critical current variations vs. temperature (Δ) = Y, (o) = Eu, (+) = Ho samples.

The Jc(0) values have been extrapolated from near liquid helium temperature data and are found in good agreement with values deduced from magnetization measurements (using Bean's formula) on unpatterned films [7].

4. Critical exponent determination

When analyzing the temperature dependence of Jc, in the vicinity of Tc in terms of a power-law variation $Jc \propto (1 - t)^n$, where $t = T/T_c$, the values of the exponent are generally found in the 1-3 range. Owing to the probable presence of insulating or normal material barriers, located at the crystalline defects, theoretical models of weakly coupled superconductors have been invoked to account for the case n = 1 [8] or n = 2 [9], the value n = 1.5 being that expected from an homogeneous superconductor in the Ginzburg-Landau description.

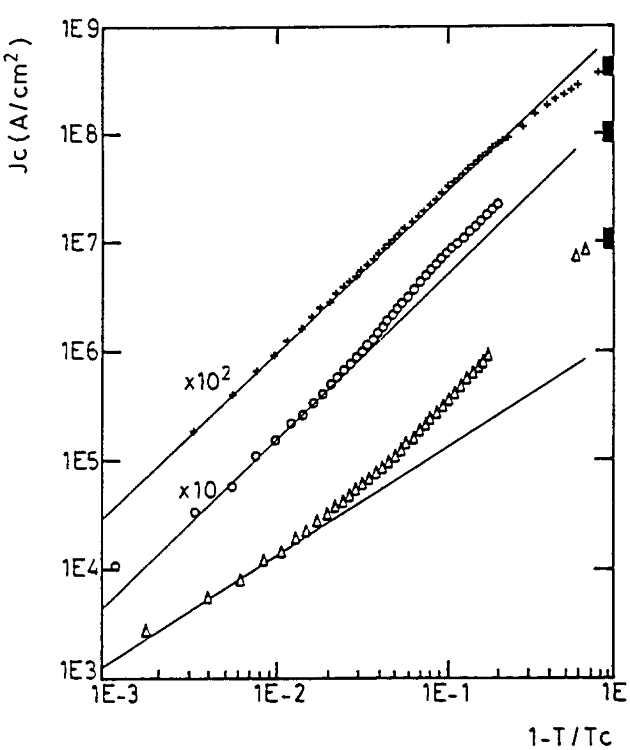

Figure 4. Fit of data with a power-law $J_c \propto (1\text{-}t)^n$ (Δ) Y : n = 1, (o) Eu : n = 1.52, (+) Ho : n = 1.49. Symbol ▮ refers to extrapolated $J_c(0)$ values.

In a more recent approach, the resulting properties of the granular nature of the HTS, specially the diamagnetic response and the critical current behaviour, have been described in the frame of phase transition of a 3D Josephson network [10, 11].

In the mean-field region, the two limits $Jc \propto (1 - t)^{3/2}$ and $Jc \propto (1 - t)$ arise naturally from this description : the first one results from the disparition of granularity as the mean field coherence length $\xi_{MF}(T)$, which is related to the mean Josephson coupling between grains and to the condensation energy, gets larger than a "grain" size *a*. In the opposite limit $\xi_{MF}(T) < a$, the system reaches a macro Josephson state. The interesting feature of this modelization lies in the description of the critical region displaying scaling-law properties where n = 2.7 when $\xi_{MF}(T) < a$, and n = 1.36 in the opposite limit, giving two more values for the critical exponents.

In Fig. 4, we plotted Jc versus (1 - t), using the experimental Tc values. Best fit of the data provides : n = 1.49 for Ho and n = 1.52 for Eu, characteristic of a homogeneous behaviour in a mean field description. Strong deviation from linearity is exhibited by the Y sample.

5. Flux pinning process

The critical current density Jc in high Tc samples is well known to be controlled by flux pinning processes. In the case of thin films it has been widely reported that defects can act as active pinning centers, thus enhancing the Jc's. Recently, spiral growth structures have been revealed by scanning tunneling microscopy (STM) on as grown surfaces of high quality c-axis YBCO thin films [12]. Screw dislocations as well as edge dislocations are thought to be a source of high density pinning sites for the case where flux lines are oriented parallel to the line of dislocation. This is especially the configuration for self-field generated flux-lines in transport-current measurements. Such spiral structures have indeed been observed on our samples [13]. In addition nano-precipitates like RE-oxides have been revealed by HRTEM observations [13] and can in the same way act as pinning centers. So we tried a different approach to analyze our expe-rimental results in the frame of the Anderson-Kim [14] flux-creep model, which describes the dynamic effects arising from the thermally activated motion of vortex lines over pinning barriers. Due to thermal excitations, flux-lines can jump over the pinning barriers with an equivalent creep velocity v depending on the pinning energy U and on the work done by the Lorentz force. Under self-field conditions this motion induces an electrical field proportional to the applied current J and to the flux-line velocity v.

In a very rough approximation [15], v can be expressed as :

$$v = v_0 \exp\left(-\frac{U}{kT}\right) \sinh\left(\frac{J \phi_0 \xi^2}{kT}\right)$$

taking for simplicity an unique length scale L ~ ξ. In the same way, we can estimate the pinning potential as : $U \propto H^2 \xi^3$ which leads (assuming Ginzburg-

Landau variations of $H_c(T)$ and $\xi(T)$) to the formal temperature dependence $U(t) = U_0\,(1+t)^{3/2}(1-t^2)^{1/2}$.

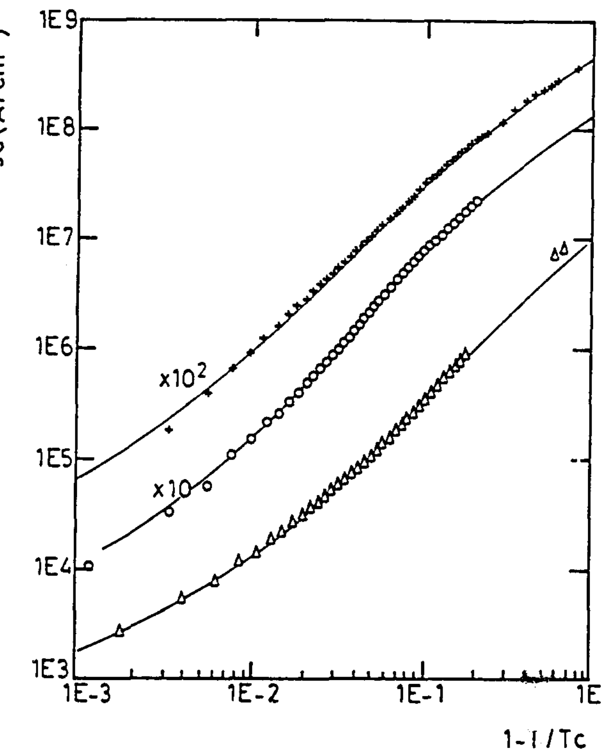

Figure 5. Fit of data with a flux - creep model
(Δ) = Y, (o) = Eu, (+) = Ho.

Using a field criterion Ec to define the critical current Jc, the latter can be determined by solving the temperature dependant implicit equation : $E_c = AJ_c v(J_c)$ where A is a constant. Theoretical fits to the data are obtained using the two adjustable parameters :

$$u_0 = \frac{U_0}{kT_c} \quad \text{and} \quad \alpha = \frac{E_c\,\Phi_0\,\xi^2_{(o)}}{A\,v_0\,kT_c}$$

Fig.5 shows the excellent agreement obtained between the calculated normalized critical current densities and the experimental points. The values of the fitting parameters are listed in Table I.

The obtained values for the pinning potential (U_0~40-80 meV) and estimations of the creep velocity (v_0~3-15 $m{\cdot}s^{-1}$) are found in the expected range.

6. Conclusion

ECP investigations have revealed the high crystalline quality of (RE)BCO laser ablation deposited films on (100)MgO substrates.

For ion-mill patterned samples, the variation of the critical current versus temperature follows two limiting dependencies of weakly coupled granular systems in a mean-field description : homogeneous superconductor for Eu and Ho samples and Josephson behaviour for the Y one.

Deviations from a power law dependence in the low temperatures range can be accounted for by a model of thermal activated vortex lines assuming a Ginzburg-Landau like dependence of the fundamental superconducting parameters.

References

1 D.B. Chrisey and A. Inam, M. R. S. Bull. 17 (1992) 37.
2 M.G. Karkut, M. Guilloux-Viry, A. Perrin, J. Padiou and M. Sergent, Physica C 179 (1989) 262.
3 A. Perrin, M.G. Karkut, M. Guilloux-Viry and M. Sergent, Appl. Phys. Lett. 58 (1991) 412.
4 M.G. Karkut, M. Guilloux-Viry, A. Perrin, C. Thivet, J. Padiou, O. Peña and M. Sergent, High T_c Superconductor Thin Films, L. Correra Ed., Elsevier Science Publ. B.V. (1992) 295.
5 A. Perrin, M. Guilloux-Viry, C. Thivet, J.C. Jegaden, M. Sergent and J. Le Lannic, Jeol News 30E (1992) 10.
6 M. Buchgeister, P. Herzog, S.M. Hosseini, K. Kopitzki and D. Wagener, Physica C 178 (1991) 105.
7 O. Peña, A. Perrin, M.G. Karkut, M. Guilloux-Viry, C. Thivet, M. Sergent, (unpublished).
8 V. Ambegaokar and A. Baratoff, Phys. Rev. Lett. 10 (1963) 486.
9 P.G. de Gennes, Rev. Mod. Phys. 36 (1964) 225 ; G. Deutscher and K.A. Müller, Phys. Rev. Lett. 59 (1987) 1745.
10 G. Deutscher, Y. Imry, Phys. Lett. 42A (1973) 413.
11 J. Rosenblatt, J.P. Burin, A. Raboutou, P. Peyral, C. Lebeau, Phase Transitions 30 (1991) 57.
12 D. G. Schlom, D. Anselmetti, J.G. Bednorz, R.F. Broom, A. Catana, T. Frey, C.H. Gerber, H.J. Güntherodt, H.P. Lang and J. Mannhart, Z. Phys. B -Condensed Matter 86 (1992) 163 ; M. McElfresh, T.G. Miller, D.M. Schaefer and R. Reifenberger, J. Appl. Phys. 71 (1992) 5099.
13 A. Catana, C. Rossel, A. Perrin, M. Guilloux-Viry and C. Thivet, EMRS fall meeting Strasbourg, 3-6 nov. 1992, submitted to J. Alloys and Compounds.
14 P.W. Anderson, Phys. Rev. Lett. 9 (1962) 309 ; P. W. Anderson and Y.B. Kim, Rev. Mod. Phys. 36 (1962) 39.
15 N. Savvides, Physica C 165 (1990) 371.